

Mathematical Modeling of Catalytic Converter Lightoff

Part II: Model Verification by Engine-Dynamometer Experiments

A transient mathematical model has been developed which describes the behavior of packed-bed catalytic converters during warmup. Model predictions agree very well with the results of engine-dynamometer experiments for three Pt-alumina catalysts of widely different properties, thus demonstrating the validity of the model.

S. H. OH and J. C. CAVENDISH

General Motors Research Laboratories
Warren, MI 48090

SCOPE

United States federal regulations of automobile exhaust emissions are based on pollutant emissions measured while driving a vehicle over a prescribed driving schedule referred to as the Federal Test Procedure (FTP). This standardized emission test procedure requires that the vehicle under test be at room temperature for a minimum of 12 h before the test. For a short period of time after the cold start, emissions of hydrocarbons and CO from the engine are quite high due to the operation of the choke. To compound the problem, the catalyst is relatively cold at this time and thus is not fully operational. As a result of the combination of the high engine-out emissions and the low catalyst efficiencies, CO and hydrocarbon emissions during the first few minutes of the FTP (i.e., warmup period) account for a large fraction of the overall FTP tailpipe emissions (Pozniak, 1980; Kummer, 1980). Consequently, improving the warmup performance of catalytic converters is an effective means of reducing CO and hydrocarbon emissions on the FTP test.

As is evident from the results of engine-dynamometer experiments presented here, catalyst properties have a strong influence on converter warmup performance. The converter models previously reported in the literature (e.g., Kuo et al., 1971; Harned, 1972; Bauerle and Nobe, 1973; Ferguson and Finlayson, 1974) were not designed to include details about the catalyst

pellets and thus are not well-suited for studying the effects of the parameters associated with catalyst design. In our previous paper (Oh et al., 1980), a detailed mathematical model was developed which describes the behavior of a single catalyst pellet under transient conditions encountered during the warmup period of automobile exhaust catalytic converters. The single-pellet model treated catalyst pellets as composite porous media composed of concentric shells of differing physical and chemical properties. Such a multilayered configuration was found to be especially convenient for examining how the lightoff behavior of a catalyst pellet is influenced by its properties, such as the poison penetration depth, and the location and width of the noble metal band.

In this paper, the second part of our converter modeling studies, we couple the single-pellet model with a mixing cell scheme to develop a mathematical model which is capable of predicting the warmup performance of the entire catalytic converter. Some of the results of model calculations presented provide useful insights into the dynamic behavior of packed-bed catalytic converters during warmup. In addition, the validity of the converter model is tested by comparing model predictions with the results of engine-dynamometer experiments for three well-characterized Pt-alumina catalysts of widely different properties.

CONCLUSIONS AND SIGNIFICANCE

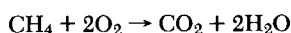
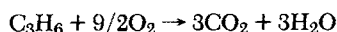
A mathematical model has been developed which describes the dynamic behavior of a packed-bed catalytic converter during its warmup period. The validity of the model was tested by comparing model predictions with engine-dynamometer test

data for General Motors production converters packed with well-characterized platinum-alumina catalyst pellets. Very good agreement was obtained between measured and calculated warmup performance, indicating that the model can be used to predict the warmup performance of packed-bed catalytic converters from specified system parameters (catalyst properties and converter dimensions) and inlet exhaust gas conditions.

The first paper in this series was published in *AIChE J.* in 1980; see the Literature Cited section for complete information.

Reaction Kinetics

In our model we consider the following oxidation reactions over Pt-alumina:



Here propylene is assumed to be representative of "fast-oxidizing hydrocarbons" in automobile exhaust and methane of "slow-oxidizing hydrocarbons" (Kuo et al., 1971). It should be noted that the consideration of only oxidation reactions does not limit the applicability of our model, because oxidizing, three-way, and dual-bed converters all may warm up in the oxidizing mode.

The following reaction rate expressions taken from Voltz et al. (1973) for the oxidation of CO, C₃H₆, and CH₄, were used in the computations.

$$\tilde{R}_{\text{CO}} = k_1 c_{\text{CO}} c_{\text{O}_2} / G \quad \text{mol CO}/(\text{cm}^2 \text{Pt} \cdot \text{s}) \quad (1)$$

$$\tilde{R}_{\text{C}_3\text{H}_6} = k_2 c_{\text{C}_3\text{H}_6} c_{\text{O}_2} / G \quad \text{mol C}_3\text{H}_6/(\text{cm}^2 \text{Pt} \cdot \text{s}) \quad (2)$$

$$\tilde{R}_{\text{CH}_4} = k_3 c_{\text{CH}_4} c_{\text{O}_2} / G \quad \text{mol CH}_4/(\text{cm}^2 \text{Pt} \cdot \text{s}) \quad (3)$$

where

$$G = (1 + K_1 c_{\text{CO}} + K_2 c_{\text{C}_3\text{H}_6})^2 \times (1 + K_3 c_{\text{CO}}^2 c_{\text{C}_3\text{H}_6}^2) / (1 + K_4 c_{\text{NO}}^{0.7}) \quad (4)$$

$$\begin{aligned} k_1 &= 6.802 \times 10^{16} \exp(-13,108/T) \\ k_2 &= 1.416 \times 10^{18} \exp(-15,109/T) \\ k_3 &= 7.443 \times 10^{13} \exp(-19,552/T) \\ K_1 &= 8.099 \times 10^6 \exp(409/T) \\ K_2 &= 2.579 \times 10^8 \exp(-191/T) \\ K_3 &= 1.13 \times 10^{21} \exp(9,299/T) \\ K_4 &= 3.02 \times 10^1 \exp(-3,733/T) \end{aligned} \quad (5)$$

We remark that the preexponential factors of the rate constants k_1 , k_2 , and k_3 in Eq. 5 were obtained by adjusting those of Voltz et al. (without changing their activation energies and adsorption equilibrium constants), based on the recycle reactor data of Schlatter and Chou (1978) to obtain the specific reaction rates (i.e., rates per unit Pt surface area). Notice that in addition to the inhibition effects of CO and C₃H₆, the adsorption term G accounts for the inhibition effect of the nonreacting species NO.

The rate of hydrogen oxidation in the exhaust gas is assumed to be the same as that for carbon monoxide. That is,

$$\tilde{R}_{\text{H}_2} = k_1 c_{\text{H}_2} c_{\text{O}_2} / G \quad \text{mol H}_2/(\text{cm}^2 \text{Pt} \cdot \text{s}) \quad (6)$$

This assumption is consistent with earlier experimental observations (Dabill et al., 1978; Stetter and Blurton, 1980) which suggest that at least in an oxidizing environment, the oxidation rates of CO and hydrogen over platinum are inhibited by CO to approximately the same extent.

From the stoichiometry, the reaction rate for oxygen is given by

$$\tilde{R}_{\text{O}_2} = 0.5\tilde{R}_{\text{CO}} + 4.5\tilde{R}_{\text{C}_3\text{H}_6} + 2\tilde{R}_{\text{CH}_4} + 0.5\tilde{R}_{\text{H}_2} \quad \text{mol O}_2/(\text{cm}^2 \text{Pt} \cdot \text{s}) \quad (7)$$

Basic Equations

The conservation of reactive species i in a spherical catalyst pellet is described by

$$\frac{1}{r^2} \frac{d}{dr} \left[D_{e,i} r^2 \frac{dc_i}{dr} \right] - a(r) \tilde{R}_i(\bar{c}, T) = 0, \quad 0 < r < R \quad (8)$$

$$i = 1(\text{CO}), 2(\text{C}_3\text{H}_6), 3(\text{CH}_4), 4(\text{H}_2), 5(\text{O}_2)$$

Note that the accumulation of mass in the catalyst pellet is neglected here in view of its small time constant (Ferguson and Finlayson, 1974). Also, the radial dependence of $a(r)$ is explicitly shown in Eq. 8 to stress the fact that the noble metal surface area is allowed to vary from one layer to another within the pellet, so that the lightoff behavior of catalyst pellets with various noble metal impregnation patterns and poison penetration depths can be readily simulated.

The boundary conditions for Eq. 8 are

$$\text{at } r = 0, \quad \frac{\partial c_i}{\partial r} = 0 \quad (9)$$

$$\text{at } r = R, \quad \frac{\partial c_i}{\partial r} = \frac{k_{m,i}}{D_{e,i}} [c_{\infty,i} - c_i] \quad (10)$$

In addition, the continuity of both the flux and concentration of the reacting species was imposed at the zone interfaces.

The energy balance equation for the catalyst pellet is

$$\rho_p C_{ps} \frac{dT}{dt} = \frac{3h}{R} [T_{\infty} - T] + \sum_{i=1}^4 (-\Delta H)_i \langle a \tilde{R}_i \rangle \quad (11)$$

subject to the initial condition

$$\text{at } t = 0, \quad T = T^{\circ} \quad (12)$$

The quantity $\langle a \tilde{R}_i \rangle$ represents the volume-averaged reaction rate defined as

$$\langle a \tilde{R}_i \rangle \equiv \frac{3}{R^3} \int_0^R a(r) \tilde{R}_i(\bar{c}, T) r^2 dr \quad (13)$$

It should be noted that the radial temperature gradient inside the catalyst pellet was neglected in deriving Eq. 11, because the validity of this uniform pellet temperature assumption in converter warmup studies has been demonstrated previously (Oh et al., 1980).

It is important to emphasize that Eqs. 8–10 are ordinary differential equations in the independent variable r with the time variable t as a parameter. This amounts to assuming that the intrapellet concentration profiles rapidly reach steady state with respect to the pellet temperature (predicted from Eqs. 11 and 12) at all times. This quasistatic assumption is valid under typical converter operating conditions because the characteristic response time for the intrapellet gas-phase concentration is much smaller than that of the pellet thermal response (Kuo et al., 1971; Ferguson and Finlayson, 1974).

The integral reactor (i.e., the entire converter) was simulated by a cascade of axial mixing cells. In the mixing cell scheme, all the catalyst pellets in a given cell are assumed to be exposed to the same bulk gas-phase condition. In view of the analysis and experiment described by Wei (1975), four layers of pellets were taken to represent a mixing cell. Since a commercial packed-bed catalytic converter is about 16 pellet diameters long (a bed depth of 5.1 cm and a pellet diameter of 0.32 cm), four mixing cells were used in the computations.

The material and energy balance equations for a mixing cell are

$$Q^{\text{in}}(c_{\infty,i}^{\text{in}} - \frac{T_{\infty}^{\text{in}}}{T_{\infty}^{\text{in}}} c_{\infty,i}^{\text{in}}) + 3k_{m,i} V_{\text{cell}} \frac{(1 - \epsilon)}{R} [c_i(R) - c_{\infty,i}] = 0 \quad (14)$$

$$W_g C_{pg} (T_{\infty}^{\text{in}} - T_{\infty}) + 3h V_{\text{cell}} \frac{(1 - \epsilon)}{R} [T - T_{\infty}] = 0 \quad (15)$$

TABLE 1. STANDARD CONDITIONS FOR MODEL CALCULATIONS

Catalyst Pellet	
0.09 wt. % Pt (60% dispersion)	
surface impregnated, 100 μm Pt band	
$R = 0.1620 \text{ cm}$	
$\rho_p = 0.776 \text{ g/cm}^3$	
$D_{e,\text{CO}} = 0.1134 \text{ cm}^2/\text{s}$	
$D_{e,\text{C}_3\text{H}_6} = 0.0791 \text{ cm}^2/\text{s}$	
$D_{e,\text{CH}_4} = 0.1346 \text{ cm}^2/\text{s}$	
$D_{e,\text{H}_2} = 0.4330 \text{ cm}^2/\text{s}$	
$D_{e,\text{O}_2} = 0.1107 \text{ cm}^2/\text{s}$	
$C_{ps} = 0.8374 \text{ J/g}\cdot\text{K}$	
$T^\circ = 300 \text{ K}$	
Converter	
Frontal Area = 516.1 cm^2	
Thickness = 5.08 cm	
$\epsilon = 0.376$	
Exhaust Gas	
$c_{g,i} = \begin{cases} 2 \text{ vol. \% CO} \\ 425 \text{ ppm C}_3\text{H}_6 \\ 150 \text{ ppm CH}_4 \\ 0.667 \text{ vol. \% H}_2 \\ 5 \text{ vol. \% O}_2 \\ 400 \text{ ppm NO} \end{cases}$	
$T_g^\circ = 550 \text{ K}$	
$W_g = 38.17 \text{ g/s}$	
$P = 101.3 \text{ kPa}$	
$C_{pg} = 1.046 \text{ J/g}\cdot\text{K}$	

Here the superscript "in" denotes the inlet value to the mixing cell of interest, whereas the variables without superscript refer to the conditions within the cell (and thus the exit conditions from the cell). Notice that the quasistatic approximation was again invoked in deriving Eqs. 14 and 15 (Ferguson and Finlayson, 1974). Also, the temperature dependence of the gas volumetric flow rate is accounted for in Eq. 14.

The external heat and mass transfer coefficients, h and $k_{m,i}$, were estimated based on the correlation of De Acetis and Thodos (1960), and their values were updated as the converter warmed up during the course of the calculations.

Numerical Solution

A detailed description of the numerical technique used to solve the single-pellet equations (Eqs. 8–13) is given in our earlier paper (Oh et al., 1980). Our approach involved the use of Galerkin's method with piecewise analytic basis functions to approximate the single-pellet equations by a well-structured nonlinear algebraic/

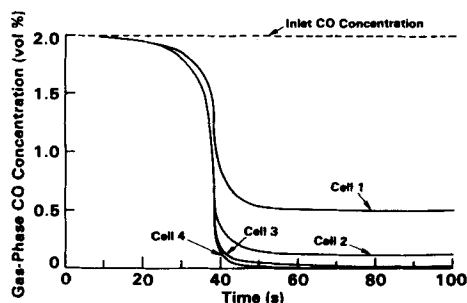


Figure 1. Time variation of bulk gas-phase CO concentration in individual cells for standard conditions, Table 1.

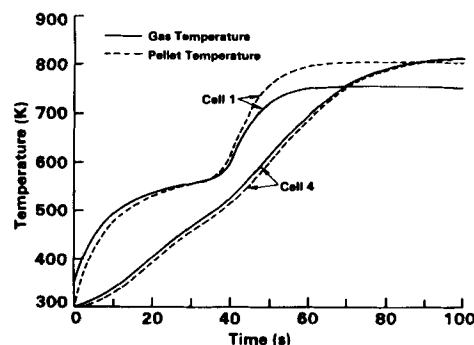


Figure 2. Time variation of gas and pellet temperatures in cells 1 and 4 for standard conditions, Table 1.

initial value problem in the time domain. The time integration of the resulting differential equations was accomplished using the GEARIB Fortran subroutine code (Hindmarsh, 1976).

Having solved the single-pellet equations, Eqs. 14 and 15 were used to calculate the exit concentrations and temperature ($c_{\infty,i}$ and T_{∞}) associated with a given cell at each time from the known inlet conditions ($c_{g,i}^{\text{in}}$ and T_g^{in}) and the solution of the single-pellet equations ($c_i(R)$ and T). Since the calculated exit concentrations and temperature constitute the inlet conditions to the next mixing cell, the same procedure was used repeatedly up to the last cell in order to predict the performance of the entire converter as a function of time.

ANALYSIS OF CONVERTER WARMUP BEHAVIOR

In this section we analyze the standard case described in Table 1 in some detail in order to gain insight into the transient response of a packed-bed converter during its warmup period. Of particular interest here is the transient response of a catalytic converter after cold catalyst pellets (300 K) are suddenly subjected to a step flow of stabilized exhaust gas at an elevated temperature (550 K). As we will see, this step increase in the exhaust temperature, though an idealization of reality, provides a valuable vehicle for understanding some of the results of engine-dynamometer experiments to be discussed later.

The catalyst properties listed in Table 1 correspond to typical low-density, alumina-supported catalyst pellets used for automobile emission control. The effective diffusivities of the reactants in the pellet were calculated from the random pore model of Wakao and Smith (Smith, 1970) using pore size distribution data. The catalyst pellets are assumed to be initially at room temperature in accordance with the cold-start procedure of the FTP test. Also, a GM type-160 packed-bed converter (which has a large frontal area and a shallow depth) was considered for the simulations. The exhaust gas composition and flow rate are similar to the test conditions of an engine dynamometer system developed for the evaluation of converter lightoff (Herod et al., 1973).

The model predicts that the conversion efficiencies at a given time decrease in the sequence of H_2 , CO , C_3H_6 , and CH_4 . In accord with the results of our previous study (Oh et al., 1980), however, the converter lightoff times (say, the time required for 50% conversion) for CO , C_3H_6 , and H_2 were predicted to be very similar because of the kinetic coupling between the species. (In all cases considered, the predicted conversion of methane was negligibly small.) For clarity, then, we will focus on the time variation of CO conversion in discussing the warmup behavior of a catalytic converter.

Figure 1 shows how the bulk gas-phase CO concentration in the individual cells of the converter varies with time, following a step increase in the exhaust temperature. (Recall that four axial mixing cells were used to simulate the entire converter.) As Figure 1 shows, the gas-phase CO concentration in the first cell (i.e., near the converter inlet) decreases rapidly near $t = 40$ s, indicating catalyst lightoff in that cell. Notice, however, that the catalyst pellets in the following cells (cells 2, 3, and 4) do not significantly shorten the time to converter lightoff; they simply improve the steady-state warmed-up performance of the converter. This prediction indicates that the time scale of converter lightoff depends primarily on the catalyst properties in the upstream section of the converter.

Figure 2 shows the corresponding time variation of the gas and pellet temperatures in cells 1 and 4 during the converter warmup period for the standard conditions listed in Table 1. It can be seen that the catalyst lightoff occurring in cell 1 near $t = 40$ s is accompanied by a rapid temperature rise in the bed above the inlet exhaust temperature (550 K). The pellet temperature in cell 1 is lower than the gas temperature for $t < 40$ s (i.e., before the catalyst lightoff), because during this period the cold pellets are heated up primarily by the convective gas-solid heat transfer. For $t > 40$ s, however, the reaction exotherm associated with the catalyst lightoff leads to a pellet temperature exceeding the gas temperature. In cell 4, on the other hand, the pellet temperature remains lower than the gas temperature throughout the transient period. This can be attributed to the fact that very little reactant is consumed in cell 4 (note the small difference between the curves for cells 3 and 4 in Figure 1) and consequently only a small amount of heat is generated as a result of the reactions.

The above finding that only the catalyst pellets near the inlet of a converter are directly responsible for converter lightoff has important implications in determining the optimum size of a catalytic converter. The predicted effects of a fourfold variation in converter volume on converter lightoff are depicted in Figure 3. In these parametric calculations, the converter volume was perturbed by varying the depth of the catalyst bed while keeping its frontal area constant at the standard value (516.1 cm²). In addition, the total amount of Pt per converter was assumed to be constant. Figure 3 shows that the lightoff time of a converter increases when a given amount of Pt is distributed over a larger catalyst volume (thereby decreasing the local Pt concentration in the catalyst bed). This is consistent with the results of Figure 1, which suggest that converter warmup time depends primarily on the local Pt concentration in the upstream section of the converter (and not on the total amount of Pt in the converter). Notice, however, that if the reaction volume is too small, the steady-state performance and poison resistance of the converter are adversely affected (Klimisch et al., 1975).

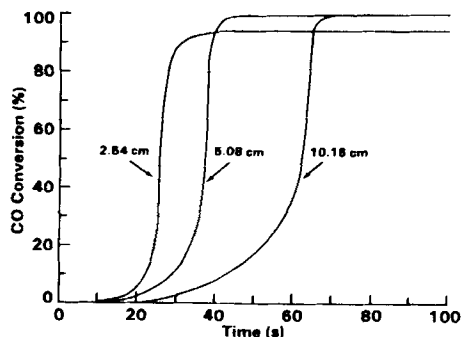


Figure 3. Effects of varying depth of converter (standard value = 5.08 cm) with frontal area and Pt content held constant. Other parameter values as in Table 1.

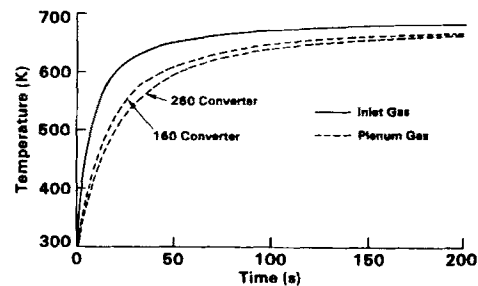


Figure 4. Time variations of inlet and plenum gas temperatures during engine-dynamometer experiment.

The model was also used to analyze the effects of other design and operating parameters on converter warmup performance by systematically perturbing them around the standard values listed in Table 1. The predicted effects of varying catalyst properties and converter operating conditions were found to be essentially the same as those reported in our previous paper (Oh et al., 1980) and thus will not be repeated here. (The single-pellet model developed in that paper describes the warmup behavior of individual catalyst pellets in one mixing cell near the converter inlet.) In view of the findings of Figure 1, this similarity in model predictions should not be surprising.

EXPERIMENTAL VERIFICATION OF THE MODEL

In order to test the validity of our converter warmup model developed here, engine-dynamometer experiments were carried out with GM production packed-bed catalytic converters. The test system has previously been described in detail by Herod et al. (1973), so only a brief description of the system will be given here.

Engine Dynamometer System

The essential elements of the test system are a test engine, a catalytic converter, and analytical instruments. Prior to each test, the catalyst was maintained at room temperature, and the exhaust gas from a 5.7 L V-8 engine was routed through the bypass line until the engine stabilized at the desired test conditions. After stability of the engine operation was achieved, the exhaust flow was suddenly directed through the catalyst bed. The converter outlet concentrations of CO and hydrocarbons (and thus their conversions) were then monitored as a function of elapsed time after the feedstream switching.

The exhaust gas compositions and flow rate for the test are the same as those given in Table 1. The exhaust temperature was measured approxi-

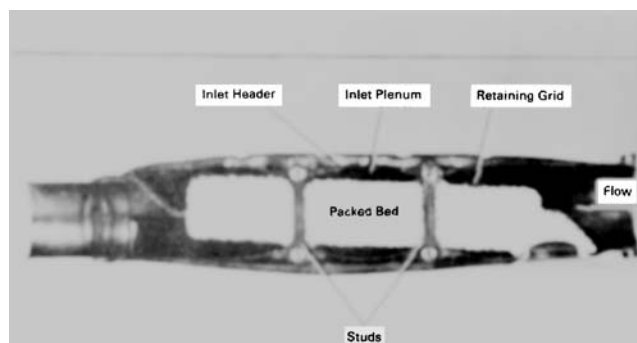


Figure 5. Cutaway view of GM packed-bed converter.

mately 20 cm upstream of the converter inlet during the test, and its time history is shown by the solid line in Figure 4.

The experiments employed two types of GM packed-bed converters having different sizes: type 160 (2.62 L) and type 260 (4.26 L). A cutaway view of a type-160 converter is shown in Figure 5. The depth of the catalyst bed for both converters is 5.08 cm; however, the frontal area of a type-260 converter (838.7 cm²) is considerably larger than that of a type-160 converter (516.1 cm²). Both the top and bottom of the converter canister are insulated to minimize heat loss to the surroundings. Since the converter is at room temperature at the beginning of the test, a significant amount of heat is transferred from the exhaust gas to the inlet header and retaining grid during converter warmup. This heat transfer causes a decrease in the temperature of the exhaust gas entering the packed bed, resulting in a delay in converter lightoff. In view of its importance in determining converter warmup performance, the time variation of the average inlet-plenum gas temperature was calculated from the measured inlet temperature (shown by the solid line in Figure 4) using a heat transfer model previously developed at GM Research Laboratories. The calculated plenum-gas temperatures for both type-160 and type-260 converters are shown by dotted lines in Figure 4 and were used as temperature inputs for our converter warmup model describing the packed bed.

Catalyst Preparation and Characterization

Three alumina-supported platinum catalysts were used in the experiments: two surface-impregnated catalysts of different Pt loadings (0.09 wt % and 0.056 wt %) and one subsurface-impregnated catalyst. All the catalysts were prepared by impregnating Grace LBD θ -alumina beads (3.24 mm diameter, 113 m²/g) using a nonaqueous method developed by D'Aniello (1983). The preparation method, which employs acetone as the impregnating solvent, allows more accurate placement of the noble metal band within the pellet than conventional aqueous procedures. The metal adsorbate solution was obtained by dissolving H₂PtCl₆·6H₂O in acetone, and for preparation of the subsurface band, sulfuric acid was applied as a blocking agent prior to introduction of the metal adsorbate solution. After impregnation, the catalysts were dried overnight and calcined in air at 500°C for 4 h.

The pore structure of the support was characterized by ultrahigh pressure mercury porosimetry ($V_{\text{macro}} = 0.366 \text{ cm}^3/\text{g}$, $V_{\text{micro}} = 0.627 \text{ cm}^3/\text{g}$, $r_{\text{macro}} = 6,962 \text{ \AA}$, $r_{\text{micro}} = 111 \text{ \AA}$). The pore size distribution data were then used to calculate the pellet density and the intrapellet effective diffusivities of the reactants. The calculated pellet density and effective diffusivities are given in Table 1. The effective diffusivities were estimated using the random pore model of Wakao and Smith (Smith, 1970) and were assumed to increase with the 1.4th power of temperature.

In order to investigate the effects of catalyst poisoning on converter lightoff, both the 0.09 wt % surface-impregnated ("Surface-Hi") and subsurface-impregnated ("Subsurface") catalysts were aged in exhaust from a 5.7 L V-8 engine (no EGR) operating at 1,800 rpm and 47 kPa manifold vacuum. During the aging, the air-fuel ratio was cycled ± 0.5 units about the stoichiometric point at 0.05 Hz. The fuel was doped with P (0.014 g P/L added as tricesyl phosphate) and Pb (0.012 g Pb/L added as tetraethyl

lead) in order to accelerate the poisoning process. The converter inlet temperature was maintained between 560 and 570°C, and the average converter bed temperature was approximately 620°C. The catalysts were aged for a total of 40 h, and after every 5 h of aging the catalyst pellets were mixed thoroughly in an attempt to ensure a uniform poison distribution within the converter. This uniform poison distribution is characteristic of the poisoning of packed-bed converters during vehicle use.

As will be discussed below, these two catalysts were found to suffer both poison penetration and thermally induced loss of active sites during the engine-dynamometer aging process. The 0.056 wt % surface-impregnated catalyst ("Surface-Lo") was thermally aged in the laboratory (18 h at 780°C in air) in order to examine the independent effect of sintering on converter lightoff.

Table 2 lists the properties of the three catalysts (both fresh and aged) used in the experiments. The CO uptakes represent a direct measure of the amount of the noble metal available for catalytic reactions. Shown are the mean and the standard deviation of three to six separate CO chemisorption measurements. For the case of the aged "Surface-Lo" catalyst, a large amount of the sample (about 20 g) was used to improve the accuracy of the CO uptake measurement. The metal dispersions were calculated from the measured CO uptakes by assuming 1:1 stoichiometry between Pt surface atoms and CO molecules. Notice that although their metal loadings are different, the fresh "Surface-Hi" and "Subsurface" catalysts contain essentially the same amount of active metal surface area, as indicated by very similar CO uptakes of these two catalysts. The location and width of the Pt band were determined from electron microprobe traces for the catalyst pellet's cross section. The mean and standard deviation of 3 pellets are listed for the "Surface-Hi" and "Surface-Lo" catalysts, while 10 pellets were analyzed for the "Subsurface" catalyst. Wet chemical analysis was used to determine the poison contents in the catalyst pellets. The poison band starts at the external surface of the pellet and its penetration depths were determined from electron microprobe observations of the pellet's cross section. Note that P penetrated into the pellet deeper than Pb; the portion of the Pt band penetrated by P was assumed to be deactivated in the calculations.

The CO uptake for the aged "Surface-Hi" catalyst was not measured because of the uncertainties involved in the interpretation of chemisorption values on catalysts exposed to engine exhaust (Dalla Betta, 1973). However, CO chemisorption measurements were made for the aged "Subsurface" catalyst because, as the results of microprobe analysis show, the poisons did not reach the subsurface Pt band. Comparison of the CO uptakes for the "Subsurface" catalyst before and after the aging shows that Pt sintered considerably (a nearly fivefold decrease in CO uptake) at the relatively mild thermal conditions encountered during the engine-dynamometer aging. Independent laboratory sintering experiments with the "Subsurface" catalyst under similar conditions (40 h at 620°C in air) showed a comparable reduction in CO uptake. In simulating the lightoff behavior of the aged "Surface-Hi" catalyst, $1/20$ of the fresh activity was assigned to the poisoned portion of the Pt band (i.e., the portion penetrated by P) in view of independent experiments with phosphorus-poisoned platinum catalysts (Hegedus and McCabe, 1981). It was also assumed that the Pt dispersion of its unpoisoned portion was reduced by the same factor as was determined from

TABLE 2. CHARACTERISTICS OF THE CATALYSTS TESTED

	Surface-Hi		Subsurface		Surface-Lo	
	Fresh	Aged	Fresh	Aged	Fresh	Aged
Pt Loading, wt. %	0.09	0.09	0.15	0.15	0.056	0.056
CO Uptake, $\mu\text{mol/g}$	2.85 ± 0.05	NM*	2.89 ± 0.03	0.63 ± 0.01	1.74 ± 0.09	0.097 ± 0.006
Pt Dispersion, %	62	14**	38	8	61	3
Pt Band						
Begins at, μm	0	0	55 ± 8	55 ± 8	0	0
Width, μm	103 ± 4	103 ± 4	75 ± 13	75 ± 13	78 ± 9	78 ± 9
Poison Content						
P, wt. %	0	0.41	0	0.34	0	0
Pb, wt. %	0	0.09	0	0.07	0	0
Poison Penetration						
P, μm	0	45	0	35	0	0
Pb, μm	0	7.5	0	8	0	0

* Not measured.

** Estimated.

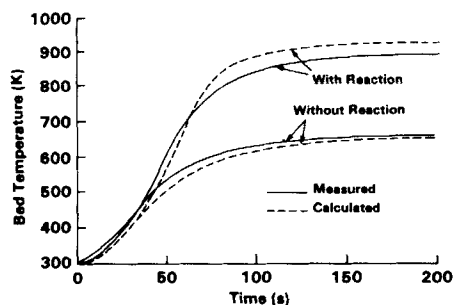


Figure 6. Comparisons of measured and calculated bed temperatures for reactive and nonreactive conditions (type-160 converter).

the CO uptakes for the fresh and aged samples of the "Subsurface" catalyst.

COMPARISON OF MODEL WITH EXPERIMENT

Since the thermal response of the packed bed plays an important role in determining the dynamic behavior of the converter system during its warmup (Kuo et al., 1971; Ferguson and Finlayson, 1974), a preliminary check on the validity of the model was made by measuring the temperature response of a type-160 converter and comparing it with model predictions for both reactive (packed with the fresh "Surface-Hi" catalyst) and nonreactive (packed with inert pellets) conditions. The gas temperature in the bed was measured using a thermocouple which was housed in a thin, perforated tube. The thermocouple was located approximately 4 cm below the top of the catalyst bed, and this corresponds to cell 4 in our model. As shown in Figure 6, reasonably good agreement was obtained between the measured and calculated thermal responses for the inert bed. This indicates that the model adequately represents the heat transfer processes occurring in GM packed-bed converters. For the case of the catalytically active bed, the model prediction is again in good agreement with the measured temperature response for $t < 50$ s. For $t > 50$ s, the model predicts a faster temperature rise followed by a higher (by 40°C) asymptotic temperature level than the experimental data. At least part of these discrepancies can be attributed to the heat loss from the converter to the surroundings, a process which was not included in our model. The larger discrepancy between the measured and predicted asymptotic temperature level observed for the reaction condition is not surprising, because the higher converter temperature attained as a result of the reaction exotherm leads to a larger amount of heat loss to the surroundings. This inability of the model to accurately predict the bed temperature at high conversion levels, however, does not interfere with the prediction of converter warmup time (say, the time to 50% CO conversion), as will be demonstrated in the sequel.

Since the primary objective of our modeling effort was to develop the ability to predict the time variation of the conversion performance during converter warmup period, a further experimental verification of the model was carried out by comparing

predicted and measured converter warmup time for the three catalysts we prepared and two different types of GM packed-bed converters. Such comparisons are made in Table 3 of the time required to achieve 50% CO conversion. Very good agreement was obtained between the model predictions and the experimental data for all the cases considered (less than 10% deviation). It is important to note that no parameters of the model were adjusted to fit the data; they were determined from independent measurements as discussed above.

Similar lightoff times observed for the fresh "Surface-Hi" and "Subsurface" catalysts (46 s vs. 48 s, both in a type-160 converter) indicate that the warmup performance of fresh converters is affected only slightly by the difference in the Pt band location considered here. (The active metal surface area was the same in both catalysts.) After being aged in engine exhaust for 40 h, however, the "Subsurface" catalyst showed substantially better warmup performance than the "Surface-Hi" catalyst (59 s vs. 67 s). This is a direct consequence of the fact that the subsurface Pt band remained unpoisoned, whereas nearly 50% of the surface band was penetrated by the poisons (see Table 2).

Comparison of the warmup times for the fresh "Surface-Hi" and "Surface-Lo" catalysts (46 s vs. 53 s, both in a type-160 converter) shows that Pt loading variations within the range of its current usage levels have a relatively moderate effect on the lightoff performance of fresh converters. As the catalysts age, however, the active metal surface area in the pellets decreases as a result of poison penetration and/or high-temperature exposure, and this in turn can cause a severe deterioration of converter warmup performance. For example, the warmup time for the "Surface-Lo" catalyst was observed to increase from 53 s to 123 s after laboratory thermal aging in air (18 h at 780°C). In addition to this increase in warmup time, converter lightoff generally becomes increasingly sensitive to the remaining active metal surface area upon catalyst aging (Oh et al., 1980). For these reasons, the initial Pt loading is an important design parameter in the development of automotive catalysts with improved durability.

As was pointed out earlier, converter warmup performance is not, in general, directly related to the total amount of Pt in the converter. This aspect is clearly demonstrated in Table 3; the warmup time for the fresh "Surface-Hi" catalyst in a type-160 converter is substantially shorter than that for the fresh "Surface-Lo" catalyst in a type-260 converter (46 s vs. 64 s) although the total amount of noble metal per converter is essentially the same for both cases. More interestingly, the "Surface-Lo" catalyst lights off considerably faster in a type-160 converter than it does in a type-260 converter (53 s vs. 64 s), despite the fact that the former converter contains less noble metal than the latter. These observations indicate that rapid converter lightoff is favored by small frontal area and high Pt concentration in the catalyst bed. The faster lightoff associated with smaller frontal area is primarily due to an increase in the gas-solid heat transfer coefficient (and consequently faster pellet warmup) resulting from the higher linear gas velocity through the catalyst bed (De Acetis and Thodos, 1960). The benefit of increasing the local Pt concentration in the upstream section of a converter can be readily understood from the results of Figure 1.

It should be mentioned that Table 3 compares the times to 50% CO conversion as determined from the CO analyzer output signal.

TABLE 3. COMPARISON OF MEASURED AND PREDICTED TIMES TO 50% CO CONVERSION

Catalyst	Converter	Fresh		Aged	
		Measured	Predicted	Measured	Predicted
Surface-Hi	160	46 s	45.7 s	67 s	66.1 s
Subsurface	160	48 s	45.8 s	59 s	58.8 s
Surface-Lo	160	53 s	49.3 s	123 s	116.5 s
Surface-Lo	260	64 s	58.8 s	—	—

This requires that the response characteristics of the analyzer system should be incorporated into the converter model in order to obtain the predicted values listed in Table 3. It is important to emphasize that the parameters associated with the analyzer dynamics were not adjusted to give a good fit to the converter warmup performance data. In the Appendix we explain in detail how the equation describing the analyzer dynamics was obtained from independent experiments and was combined with the converter warmup model to calculate the predicted warmup times listed in Table 3.

CONCLUSION

This study has shown that our model, despite the simplifying assumptions invoked in the development (e.g., flow uniformity in the packed bed, no heat loss from the converter to the surroundings), describes the essential features of a packed-bed catalytic converter well enough to permit the quantitative prediction of its warmup performance during engine-dynamometer tests. In addition to providing a predictive tool, the model improves our understanding of the dynamic behavior of a catalytic converter during warmup.

In a subsequent paper (Oh and Cavendish, 1985), the converter warmup model developed here will be applied to the first two cycles of the FTP in order to evaluate its capability to predict the tailpipe emissions during the cold-start portion of actual vehicle emission tests. The results of parametric calculations will also be presented which quantify the effects of catalyst/converter design parameters on cold-start exhaust emissions.

ACKNOWLEDGMENT

The authors gratefully acknowledge the technical help of the following members of the GM Research Laboratories: J. Carpenter (catalyst preparation and characterization), S. Whittington (CO chemisorption measurements), and R. Richmond (accelerated catalyst poisoning) of the Physical Chemistry Department. A. Ottolini of the Analytical Chemistry Department provided the electron microprobe data. The plenum gas temperatures in Figure 4 were computed by G. Robertson of the Engine Research Department. Thanks also go to J. Smith and J. Leptich of the AC Spark Plug Division for providing the data of engine-dynamometer experiments.

APPENDIX

In our test system, the concentration signal was found to be significantly distorted between the converter outlet and analyzer output. It was assumed that the nonidealities associated with the concentration measurements are composed of two basic components: pure time delay (e.g., the transportation lag in the pipeline connecting the converter and the analyzers) and mixing chamber distortion (e.g., signal dispersion due to gas-phase mixing in the pipeline as well as within the analyzer). Under this assumption the analyzer output signal $y(t)$ can be related to the actual concentration at the converter outlet $x(t)$ by the following simple differential equation:

$$\theta \frac{dy(t)}{dt} + y(t) = x(t - \tau) \quad (A1)$$

In order to determine the parameters θ and τ for the CO concentration measurements, the output signal of the CO analyzer was monitored as a function of time after introducing a step increase in the CO concentration at the converter outlet. A least-squares fit

of θ and τ based on the measured step response (i.e., y vs. t) yielded $\theta = 0.9$ s and $\tau = 6.0$ s at the gas flow rate employed in our engine-dynamometer tests.

Having determined the values of θ and τ , the observed time variation of CO concentration $y(t)$ was calculated from Eq. A1 using as the forcing function $x(t - \tau)$, the converter outlet concentration predicted by our warmup model. The predicted warmup times listed in Table 3 were then determined from the calculated $y(t)$.

NOTATION

a	= local platinum surface area, cm ² Pt/cm ³ pellet
c_i	= concentration of reactive species i in the catalyst pellet, mol/cm ³
c_{NO}	= NO concentration in the catalyst pellet, ppm
\vec{c}	= vector whose entries are species concentrations c_i
$c_{\infty, i}$	= concentration of species i in the bulk gas phase of the mixing cell, or concentration of species i in the gas stream leaving the mixing cell, mol/cm ³
$c_{i, \infty}^{\text{in}}$	= concentration of species i in the gas stream entering the mixing cell, mol/cm ³
$c_{g, i}$	= concentration of species i in the exhaust gas at the converter inlet, vol.% or ppm
C_{pg}	= heat capacity of gas, J/g·K
C_{ps}	= heat capacity of catalyst pellet, J/g·K
$D_{e, i}$	= effective diffusivity of species i in the catalyst pellet, cm ² /s
G	= quantity defined by Eq. 4
h	= heat transfer coefficient, J/cm ² ·s·K
$(-\Delta H)_i$	= heat of combustion of species i , J/mol
k_i	= rate constant for reaction i , cm ⁴ /s·mol
$k_{m, i}$	= mass transfer coefficient of species i , cm/s
K_i	= adsorption equilibrium constant for species i
P	= pressure, kPa
Q^{in}	= volumetric flow rate of the gas entering the mixing cell, cm ³ /s
r	= pellet radial coordinate, cm
\bar{r}_{macro}	= integral-averaged macropore radius, Å
\bar{r}_{micro}	= integral-averaged micropore radius, Å
R	= radius of a spherical catalyst pellet, cm
\bar{R}_i	= specific reaction rate for species i , mol/cm ² Pt·s
t	= time, s
T	= temperature in the catalyst pellet, K
T°	= initial pellet temperature, K
T_∞	= temperature of the bulk gas phase in the mixing cell, or temperature of the gas stream leaving the mixing cell, K
T_∞^{in}	= temperature of the gas stream entering the mixing cell, K
T_g	= exhaust gas temperature at the converter inlet, K
V_{cell}	= volume of a mixing cell, cm ³
V_{macro}	= pellet macropore volume, cm ³ /g
V_{micro}	= pellet micropore volume, cm ³ /g
W_g	= mass flow rate of exhaust gas, g/s
x	= actual concentration at the converter outlet, vol.% or mol/cm ³
y	= analyzer output signal, vol.% or mol/cm ³

Greek Letters

ϵ	= bed void fraction
θ	= time constant of the analyzer system, s
ρ_p	= pellet density, g/cm ³
τ	= transportation lag in the analyzer system, s

LITERATURE CITED

- Bauerle, G. L., and K. Nobe, "Two-Stage Catalytic Converter: Transient Operation," *Ind. Eng. Chem. Proc. Des. Dev.*, **12**, 407 (1973).
- Dabill, D. W., et al., "The Oxidation of Hydrogen and Carbon Monoxide Mixture Over Platinum," *J. Catal.*, **53**, 164 (1978).
- Dalla Betta, R. A., "Hydrogen-Oxygen Titration of Surface Platinum in Poisoning Studies," *J. Catal.*, **31**, 143 (1973).
- D'Aniello, Jr., M. J., "Method of Making Layered Catalysts," U.S. Patent 4,380,510, General Motors Res. Labs., Warren, MI (1983).
- De Acetis, J., and G. Thodos, "Flow of Gases Through Spherical Packings," *Ind. Eng. Chem.*, **52**, 1,003 (1960).
- Ferguson, N. B., and B. A. Finlayson, "Transient Modeling of a Catalytic Converter to Reduce Nitric Oxide in Automobile Exhaust," *AIChE J.*, **20**, 540 (1974).
- Harned, J. L., "Analytical Evaluation of a Catalytic Converter System," *SAE Paper* 720,520 (1972).
- Hegedus, L. L., and R. W. McCabe, "Catalyst Poisoning," *Catal. Rev.-Sci. Eng.*, **23**, 377 (1981).
- Herod, D. M., M. V. Nelson, and W. M. Wang, "An Engine Dynamometer System for the Measurement of Converter Performance," *SAE Paper* 730,557 (1973).
- Hindmarsh, A. C., "GEARIB, Solution of Implicit Systems of Ordinary Differential Equations with Banded Jacobian," *Lawrence Livermore Lab. Rpt. UCID 30,130* (Feb., 1976).
- Klimisch, R. L., J. C. Summers, and J. C. Schlatter, "The Chemistry of Degradation in Automotive Emission Control Catalysts," *Adv. Chem. Ser.*, **143**, 103 (1975).
- Kummer, J. T., "Catalysts for Automobile Emission Control," *Prog. Energy Combust. Sci.*, **6**, 177 (1980).
- Kuo, J. C. W., C. R. Morgan, and H. G. Lassen, "Mathematical Modeling of CO and HC Catalytic Converter Systems," *SAE Paper* 710,289 (1971).
- Oh, S. H., J. C. Cavendish, and L. L. Hegedus, "Mathematical Modeling of Catalytic Converter Lightoff: Single-Pellet Studies," *AIChE J.*, **26**, 935 (1980).
- Oh, S. H., and J. C. Cavendish, "Mathematical Modeling of Catalytic Converter Lightoff: Part III. Prediction of Vehicle Exhaust Emissions and Parametric Analysis," *AIChE J.* (1985).
- Pozniak, D. J., "The Exhaust Emission and Fuel Consumption Characteristics of an Engine During Warmup—A Vehicle Study," *SAE Paper* 800,396 (1980).
- Schlatter, J. C., and T. S. Chou, "Measuring Oxidation Rates in a Recycle Reactor," *AIChE 71st Ann. Meet.*, Paper No. 66f, Miami Beach (Nov., 1978).
- Smith, J. M., *Chemical Engineering Kinetics*, McGraw-Hill, New York (1970).
- Stetter, J. R., and K. F. Blurton, "Catalytic Oxidation of CO and H₂ Mixtures in Air," *Ind. Eng. Chem. Prod. Res. Dev.*, **19**, 214 (1980).
- Voltz, S. E., et al., "Kinetic Study of Carbon Monoxide and Propylene Oxidation on Platinum Catalysts," *Ind. Eng. Chem. Prod. Res. Dev.*, **12**, 294 (1973).
- Wei, J., "Catalysis for Motor Vehicle Emissions," *Adv. Catal.*, **24**, 57 (1975).

Manuscript received June 14, 1984; revision received Oct. 25, and accepted Oct. 29.